WEIGHTED BELLMAN BACKUPS FOR IMPROVED SIGNAL-TO-NOISE IN Q-UPDATES

Anonymous authors
Paper under double-blind review

ABSTRACT

Off-policy deep reinforcement learning (RL) has been successful in a range of challenging domains. However, standard off-policy RL algorithms can suffer from low signal and even instability in Q-learning because target values are derived from current Q-estimates, which are often noisy. To mitigate the issue, we propose ensemble-based weighted Bellman backups, which re-weight target Q-values based on uncertainty estimates from a Q-ensemble. We empirically observe that the proposed method stabilizes and improves learning on both continuous and discrete control benchmarks. We also specifically investigate the signal-to-noise aspect by studying environments with noisy rewards, and find that weighted Bellman backups significantly outperform standard Bellman backups. Furthermore, since our weighted Bellman backups rely on maintaining an ensemble, we investigate how weighted Bellman backups interact with other benefits previously derived from ensembles: (a) Bootstrap; (b) UCB Exploration. We show that these different ideas are largely orthogonal and can be fruitfully integrated, together further improving the performance of existing off-policy RL algorithms, such as Soft Actor-Critic and Rainbow DQN, for both continuous and discrete control tasks on both low-dimensional and high-dimensional environments.

1 INTRODUCTION

Model-free reinforcement learning (RL), with high-capacity function approximators, such as deep neural networks (DNNs), has been used to solve a variety of sequential decision-making problems, including board games (Silver et al., 2017; 2018), video games (Mnih et al., 2015; Vinyals et al., 2019), and robotic manipulation (Kalashnikov et al., 2018). It has been well established that the above successes are highly sample *inefficient* (Kaiser et al., 2020). Recently, a lot of progress has been made in more sample-efficient model-free RL algorithms through improvements in off-policy learning both in discrete and continuous domains (Fujimoto et al., 2018; Haarnoja et al., 2018; Hessel et al., 2018; Amos et al., 2020). However, standard off-policy RL algorithms can suffer from instability in Q-learning due to error propagation in the Bellman backup, i.e., the errors induced in the target value can lead to an increase in overall error in the Q-function (Kumar et al., 2019; 2020).

One way to address the error propagation issue is to use ensemble methods, which combine multiple models of the value function (Hasselt, 2010; Van Hasselt et al., 2016; Fujimoto et al., 2018). For discrete control tasks, double Q-learning (Hasselt, 2010; Van Hasselt et al., 2016) addressed the value overestimation by maintaining two independent estimators of the action values and later extended to continuous control tasks in TD3 (Fujimoto et al., 2018). While most prior work has improved the stability by taking the minimum over Q-functions, this also needlessly loses signal, and we propose an alternative way that utilizes ensembles to estimate uncertainty and provide more stable, higher-signal-to-noise backups.

In this paper, we propose ensemble-based weighted Bellman backups that can be applied to most modern off-policy RL algorithms, such as Q-learning and actor-critic algorithms. Our main idea is to reweight sample transitions based on uncertainty estimates from a Q-ensemble. Because prediction errors can be characterized by uncertainty estimates from ensembles (i.e., variance of predictions) as shown in Figure 1(b), we find that the proposed method significantly improves the signal-to-noise in the Q-updates and stabilizes the learning process. Finally, we present a unified framework, coined SUNRISE, that combines our weighted Bellman backups with (a) bootstrap with

random initialization that improves the diversity of ensemble agents (Osband et al., 2016), and (b) an inference method that selects actions using highest upper-confidence bounds (UCB) for efficient exploration (Chen et al., 2017). We find that these different ideas can be fruitfully integrated, and they are largely complementary (see Figure 1(a)).

We demonstrate the effectiveness of the proposed method using Soft Actor-Critic (SAC; Haarnoja et al. 2018) for continuous control benchmarks (specifically, OpenAI Gym (Brockman et al., 2016) and DeepMind Control Suite (Tassa et al., 2018)) and Rainbow DQN (Hessel et al., 2018) for discrete control benchmarks (specifically, Atari games (Bellemare et al., 2013)). In our experiments, SUNRISE consistently improves the performance of existing off-policy RL methods. Furthermore, we find that the proposed weighted Bellman backups yield improvements in environments with noisy reward, which have a low signal-to-noise ratio.

2 Related work

Off-policy RL algorithms. Recently, various off-policy RL algorithms have provided large gains in sample-efficiency by reusing past experiences (Fujimoto et al., 2018; Haarnoja et al., 2018; Hessel et al., 2018). Rainbow DQN (Hessel et al., 2018) achieved state-of-the-art performance on the Atari games (Bellemare et al., 2013) by combining several techniques, such as double Q-learning (Van Hasselt et al., 2016) and distributional DQN (Bellemare et al., 2017). For continuous control tasks, SAC (Haarnoja et al., 2018) achieved state-of-the-art sample-efficiency results by incorporating the maximum entropy framework. Our ensemble method brings orthogonal benefits and is complementary and compatible with these existing state-of-the-art algorithms.

Stabilizing Q-learning. It has been empirically observed that instability in Q-learning can be caused by applying the Bellman backup on the learned value function (Hasselt, 2010; Van Hasselt et al., 2016; Fujimoto et al., 2018; Kumar et al., 2019; 2020). By following the principle of double Q-learning (Hasselt, 2010; Van Hasselt et al., 2016), twin-Q trick (Fujimoto et al., 2018) was proposed to handle the overestimation of value functions for continuous control tasks. Recently, Kumar et al. (2020) handled the error propagation issue by reweighting the Bellman backup based on cumulative Bellman errors. However, our method is different in that we propose an alternative way that also utilizes ensembles to estimate uncertainty and provide more stable, higher-signal-to-noise backups.

Ensemble methods in RL. Ensemble methods have been studied for different purposes in RL (Wiering & Van Hasselt, 2008; Osband et al., 2016; Anschel et al., 2017; Agarwal et al., 2020; Lan et al., 2020). Chua et al. (2018) showed that modeling errors in model-based RL can be reduced using an ensemble of dynamics models, and Kurutach et al. (2018) accelerated policy learning by generating imagined experiences from the ensemble of dynamics models. Bootstrapped DQN (Osband et al., 2016) leveraged the ensemble of Q-functions for efficient exploration. However, most prior works have studied the various axes of improvements from ensemble methods in isolation, while we propose a unified framework that handles various issues in off-policy RL algorithms.

Exploration in RL. To balance exploration and exploitation, several methods, such as the maximum entropy frameworks (Ziebart, 2010; Haarnoja et al., 2018) and exploration bonus rewards (Bellemare et al., 2016; Houthooft et al., 2016; Pathak et al., 2017; Choi et al., 2019), have been proposed. Despite the success of these exploration methods, a potential drawback is that agents can focus on irrelevant aspects of the environment because these methods do not depend on the rewards. To handle this issue, Chen et al. (2017) proposed an exploration strategy that considers both best estimates (i.e., mean) and uncertainty (i.e., variance) of Q-functions for discrete control tasks. We further extend this strategy to continuous control tasks and show that it can be combined with other techniques.

3 Background

Reinforcement learning. We consider a standard RL framework where an agent interacts with an environment in discrete time. Formally, at each timestep t, the agent receives a state s_t from the environment and chooses an action a_t based on its policy π. The environment returns a reward r_t and the agent transitions to the next state s_{t+1}. The return $R_t = \sum_{k=0}^{\infty} \gamma^k r_{t+k}$ is the total accumulated rewards from timestep t with a discount factor $\gamma \in [0, 1)$. RL then maximizes the expected return from each state s_t.

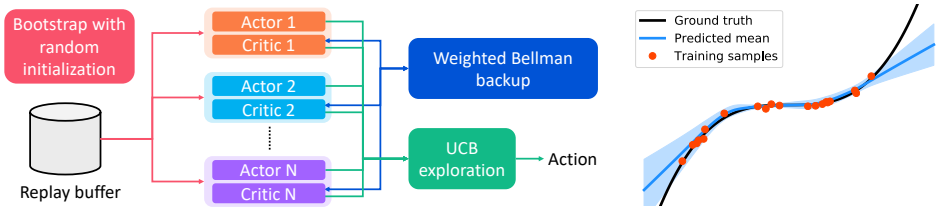

(a) SUNRISE: actor-critic version (b) Uncertainty estimates

Figure 1: (a) Illustration of our framework. We consider N independent agents (i.e., no shared parameters between agents) with one replay buffer. (b) Uncertainty estimates from an ensemble of neural networks on a toy regression task (see Appendix C for more experimental details). The black line is the ground truth curve, and the red dots are training samples. The blue lines show the mean and variance of predictions over ten ensemble models. The ensemble can produce well-calibrated uncertainty estimates (i.e., variance) on unseen samples.

Soft Actor-Critic. SAC (Haarnoja et al., 2018) is an off-policy actor-critic method based on the maximum entropy RL framework (Ziebart, 2010), which encourages the robustness to noise and exploration by maximizing a weighted objective of the reward and the policy entropy (see Appendix A for further details). To update the parameters, SAC alternates between a soft policy evaluation and a soft policy improvement. At the soft policy evaluation step, a soft Q-function, which is modeled as a neural network with parameters θ, is updated by minimizing the following soft Bellman residual:

$$\mathcal{L}^{\texttt{SAC}}_{\texttt{critic}}(\theta) = \mathbb{E}_{\tau_t \sim \mathcal{B}}[\mathcal{L}_Q(\tau_t, \theta)], \tag{1}$$

$$\mathcal{L}_Q(\tau_t, \theta) = \left(Q_\theta(s_t, a_t) - r_t - \gamma \mathbb{E}_{a_{t+1} \sim \pi_\phi}\left[Q_{\bar{\theta}}(s_{t+1}, a_{t+1}) - \alpha \log \pi_\phi(a_{t+1}|s_{t+1})\right]\right)^2, \tag{2}$$

where $\tau_t = (s_t, a_t, r_t, s_{t+1})$ is a transition, $\mathcal{B}$ is a replay buffer, $\bar{\theta}$ are the delayed parameters, and α is a temperature parameter. At the soft policy improvement step, the policy π with its parameter ϕ is updated by minimizing the following objective:

$$\mathcal{L}^{\texttt{SAC}}_{\texttt{actor}}(\phi) = \mathbb{E}_{s_t \sim \mathcal{B}}\left[\mathcal{L}_\pi(s_t, \phi)\right], \text{ where } \mathcal{L}_\pi(s_t, \phi) = \mathbb{E}_{a_t \sim \pi_\phi}\left[\alpha \log \pi_\phi(a_t|s_t) - Q_\theta(s_t, a_t)\right]. \tag{3}$$

Here, the policy is modeled as a Gaussian with mean and covariance given by neural networks to handle continuous action spaces.

4 SUNRISE

In this section, we propose the ensemble-based weighted Bellman backups, and then introduce SUNRISE: **S**imple **UN**ified framework for **Re**I**nforcement** learning using en**SE**mbles, which combines various ensemble methods. In principle, our method can be used in conjunction with most modern off-policy RL algorithms, such as SAC (Haarnoja et al., 2018) and Rainbow DQN (Hessel et al., 2018). For the exposition, we describe only the SAC version in the main body. The Rainbow DQN version follows the same principles and is fully described in Appendix B.

4.1 Weighted Bellman backups to improve signal-to-noise in Q-updates

Formally, we consider an ensemble of N SAC agents, i.e., $\{Q_{\theta_i}, \pi_{\phi_i}\}_{i=1}^N$, where θ_i and ϕ_i denote the parameters of the i-th soft Q-function and policy.[1] Since conventional Q-learning is based on the Bellman backup in (2), it can be affected by error propagation. I.e., error in the target Q-function $Q_{\bar{\theta}}(s_{t+1}, a_{t+1})$ gets propagated into the Q-function $Q_\theta(s_t, a_t)$ at the current state. Recently, Kumar et al. (2020) showed that this error propagation can cause inconsistency and unstable convergence. To mitigate this issue, for each agent i, we consider a weighted Bellman backup as follows:

$$\begin{aligned}&\mathcal{L}_{WQ}(\tau_t, \theta_i) \\ &= w(s_{t+1}, a_{t+1})\left(Q_{\theta_i}(s_t, a_t) - r_t - \gamma\left(Q_{\bar{\theta}_i}(s_{t+1}, a_{t+1}) - \alpha \log \pi_\phi(a_{t+1}|s_{t+1})\right)\right)^2,\end{aligned} \tag{4}$$

[1] We remark that each Q-function $Q_{\theta_i}(s, a)$ has a unique target Q-function $Q_{\bar{\theta}_i}(s, a)$.

where $\tau_t = (s_t, a_t, r_t, s_{t+1})$ is a transition, $a_{t+1} \sim \pi_\phi(a|s_t)$, and $w(s,a)$ is a confidence weight based on ensemble of target Q-functions:

$$w(s,a) = \sigma\left(-\bar{Q}_{\texttt{std}}(s,a) * T\right) + 0.5, \tag{5}$$

where $T > 0$ is a temperature, σ is the sigmoid function, and $\bar{Q}_{\texttt{std}}(s,a)$ is the empirical standard deviation of all target Q-functions $\{Q_{\bar{\theta}_i}\}_{i=1}^N$. Note that the confidence weight is bounded in $[0.5, 1.0]$ because standard deviation is always positive.[2] The proposed objective $\mathcal{L}_{WQ}$ down-weights the sample transitions with high variance across target Q-functions, resulting in a loss function for the Q-updates that has a better signal-to-noise ratio.

4.2 Combination with additional techniques that leverage ensembles

To further improve the performance, we integrate the proposed weighted Bellman backup with previous techniques that use ensembles (i.e., bootstrap and UCB exploration) into a single framework.

Bootstrap with random initialization. To train the ensemble of agents, we use the bootstrap with random initialization (Efron, 1982; Osband et al., 2016), which enforces the diversity between agents through two simple ideas: First, we initialize the model parameters of all agents with random parameter values for inducing an initial diversity in the models. Second, we apply different samples to train each agent. Specifically, for each SAC agent i in each timestep t, we draw the binary masks $m_{t,i}$ from the Bernoulli distribution with parameter $\beta \in (0, 1]$, and store them in the replay buffer. Then, when updating the model parameters of agents, we multiply the bootstrap mask to each objective function, such as: $m_{t,i}\mathcal{L}_\pi(s_t, \phi_i)$ and $m_{t,i}\mathcal{L}_{WQ}(\tau_t, \theta_i)$ in (3) and (4), respectively. We remark that Osband et al. (2016) applied this simple technique to train an ensemble of DQN (Mnih et al., 2015) only for discrete control tasks, while we apply to SAC (Haarnoja et al., 2018) and Rainbow DQN (Hessel et al., 2018) for both continuous and discrete tasks with additional techniques.

UCB exploration. The ensemble can also be leveraged for efficient exploration (Chen et al., 2017; Osband et al., 2016) because it can express higher uncertainty on unseen samples. Motivated by this, by following the idea of Chen et al. (2017), we consider an optimism-based exploration that chooses the action that maximizes

$$a_t = \max_a \{Q_{\texttt{mean}}(s_t, a) + \lambda Q_{\texttt{std}}(s_t, a)\}, \tag{6}$$

where $Q_{\texttt{mean}}(s,a)$ and $Q_{\texttt{std}}(s,a)$ are the empirical mean and standard deviation of all Q-functions $\{Q_{\theta_i}\}_{i=1}^N$, and the $\lambda > 0$ is a hyperparameter. This inference method can encourage exploration by adding an exploration bonus (i.e., standard deviation $Q_{\texttt{std}}$) for visiting unseen state-action pairs similar to the UCB algorithm (Auer et al., 2002). We remark that this inference method was originally proposed in Chen et al. (2017) for efficient exploration in discrete action spaces. However, in continuous action spaces, finding the action that maximizes the UCB is not straightforward. To handle this issue, we propose a simple approximation scheme, which first generates N candidate action set from ensemble policies $\{\pi_{\phi_i}\}_{i=1}^N$, and then chooses the action that maximizes the UCB (Line 4 in Algorithm 1). For evaluation, we approximate the maximum a posterior action by averaging the mean of Gaussian distributions modeled by each ensemble policy.

The full procedure of our unified framework, coined SUNRISE, is summarized in Algorithm 1.

5 Experimental results

We designed our experiments to answer the following questions:

- Can SUNRISE improve off-policy RL algorithms, such as SAC (Haarnoja et al., 2018) and Rainbow DQN (Hessel et al., 2018), for both continuous (see Table 1 and Table 2) and discrete (see Table 3) control tasks?
- How crucial is the proposed weighted Bellman backups in (4) for improving the signal-to-noise in Q-updates (see Figure 2)?
- Can UCB exploration be useful for solving tasks with sparse rewards (see Figure 3(a))?
- Is SUNRISE better than a single agent with more updates and parameters (see Figure 3(b))?
- How does ensemble size affect the performance (see Figure 3(c))?

[2] We find that it is empirically stable to set minimum value of weight $w(s,a)$ as 0.5.

Algorithm 1 SUNRISE: SAC version

for each iteration **do**
  for each timestep t **do**
    // UCB EXPLORATION
    Collect N action samples: $\mathcal{A}_t = \{a_{t,i} \sim \pi_{\phi_i}(a|s_t) | i \in \{1, \ldots, N\}\}$
    Choose the action that maximizes UCB: $a_t = \underset{a_{t,i} \in \mathcal{A}_t}{\arg\max}\ Q_{\texttt{mean}}(s_t, a_{t,i}) + \lambda Q_{\texttt{std}}(s_t, a_{t,i})$
    Collect state s_{t+1} and reward r_t from the environment by taking action a_t
    Sample bootstrap masks $M_t = \{m_{t,i} \sim \text{Bernoulli}\,(\beta) — i \in \{1, \ldots, N\}\}$
    Store transitions $\tau_t = (s_t, a_t, s_{t+1}, r_t)$ and masks in replay buffer $\mathcal{B} \leftarrow \mathcal{B} \cup \{(\tau_t, M_t)\}$
  end for
  // UPDATE AGENTS VIA BOOTSTRAP AND WEIGHTED BELLMAN BACKUP
  for each gradient step **do**
    Sample random minibatch $\{(\tau_j, M_j)\}_{j=1}^{B} \sim \mathcal{B}$
    for each agent i **do**
      Update the Q-function by minimizing $\frac{1}{B}\sum_{j=1}^{B} m_{j,i}\mathcal{L}_{WQ}(\tau_j, \theta_i)$ in (4)
      Update the policy by minimizing $\frac{1}{B}\sum_{j=1}^{B} m_{j,i}\mathcal{L}_{\pi}(s_j, \phi_i)$ in (3)
    end for
  end for
end for

5.1 SETUPS

Continuous control tasks. We evaluate SUNRISE on several continuous control tasks using simulated robots from OpenAI Gym (Brockman et al., 2016) and DeepMind Control Suite (Tassa et al., 2018). For OpenAI Gym experiments with proprioceptive inputs (e.g., positions and velocities), we compare to PETS (Chua et al., 2018), a state-of-the-art model-based RL method based on ensembles of dynamics models; POPLIN-P (Wang & Ba, 2020), a state-of-the-art model-based RL method which uses a policy network to generate actions for planning; POPLIN-A (Wang & Ba, 2020), variant of POPLIN-P which adds noise in the action space; METRPO (Kurutach et al., 2018), a hybrid RL method which augments TRPO (Schulman et al., 2015) using ensembles of dynamics models; and two state-of-the-art model-free RL methods, TD3 (Fujimoto et al., 2018) and SAC (Haarnoja et al., 2018). For our method, we consider a combination of SAC and SUNRISE, as described in Algorithm 1. Following the setup in Wang & Ba (2020) and Wang et al. (2019), we report the mean and standard deviation across ten runs after 200K timesteps on five complex environments: Cheetah, Walker, Hopper, Ant and SlimHumanoid with early termination (ET). More experimental details and learning curves with 1M timesteps are in Appendix D.

For DeepMind Control Suite with image inputs, we compare to PlaNet (Hafner et al., 2019), a model-based RL method which learns a latent dynamics model and uses it for planning; Dreamer (Hafner et al., 2020), a hybrid RL method which utilizes the latent dynamics model to generate synthetic roll-outs; SLAC (Lee et al., 2020), a hybrid RL method which combines the latent dynamics model with SAC; and three state-of-the-art model-free RL methods which apply contrastive learning (CURL; Srinivas et al. 2020) or data augmentation (RAD (Laskin et al., 2020) and DrQ (Kostrikov et al., 2020)) to SAC. For our method, we consider a combination of RAD (i.e., SAC with random crop) and SUNRISE. Following the setup in RAD, we report the mean and standard deviation across five runs after 100k (i.e., low sample regime) and 500k (i.e., asymptotically optimal regime) environment steps on six environments: Finger-spin, Cartpole-swing, Reacher-easy, Cheetah-run, Walker-walk, and Cup-catch. More experimental details and learning curves are in Appendix F.

Discrete control benchmarks. For discrete control tasks, we demonstrate the effectiveness of SUNRISE on several Atari games (Bellemare et al., 2013). We compare to SimPLe (Kaiser et al., 2020), a hybrid RL method which updates the policy only using samples generated by learned dynamics model; Rainbow DQN (Hessel et al., 2018) with modified hyperparameters for sample-efficiency (van Hasselt et al., 2019); Random agent (Kaiser et al., 2020); two state-of-the-art model-free RL methods which apply the contrastive learning (CURL; Srinivas et al. 2020) and data augmentation (DrQ; Kostrikov et al. 2020) to Rainbow DQN; and Human performances reported in Kaiser et al. (2020) and van Hasselt et al. (2019). Following the setups in SimPLe, we report the mean across

	Cheetah	Walker	Hopper	Ant	SlimHumanoid-ET
PETS	2288.4 ± 1019.0	282.5 ± 501.6	114.9 ± 621.0	1165.5 ± 226.9	**2055.1 ± 771.5**
POPLIN-A	1562.8 ± 1136.7	-105.0 ± 249.8	202.5 ± 962.5	1148.4 ± 438.3	-
POPLIN-P	4235.0 ± 1133.0	597.0 ± 478.8	2055.2 ± 613.8	**2330.1 ± 320.9**	-
METRPO	2283.7 ± 900.4	-1609.3 ± 657.5	1272.5 ± 500.9	282.2 ± 18.0	76.1 ± 8.8
TD3	3015.7 ± 969.8	-516.4 ± 812.2	1816.6 ± 994.8	870.1 ± 283.8	1070.0 ± 168.3
SAC	4474.4 ± 700.9	299.5 ± 921.9	1781.3 ± 737.2	979.5 ± 253.2	1371.8 ± 473.4
SUNRISE	**4501.8 ± 443.8**	**1236.5 ± 1123.9**	**2643.2 ± 472.3**	1502.4 ± 483.5	1926.6 ± 375.0

Table 1: Performance on OpenAI Gym at 200K timesteps. The results show the mean and standard deviation averaged over ten runs, and the best results are indicated in bold. For baseline methods, we report the best number in prior works (Wang & Ba, 2020; Wang et al., 2019).

500K step	PlaNet	Dreamer	SLAC	CURL	DrQ	RAD	SUNRISE
Finger-spin	561 ± 284	796 ± 183	673 ± 92	926 ± 45	938 ± 103	975 ± 16	**983** ±1
Cartpole-swing	475 ± 71	762 ± 27	-	845 ± 45	868 ± 10	873 ± 3	**876** ± 4
Reacher-easy	210 ± 44	793 ± 164	-	929 ± 44	942 ± 71	916 ± 49	**982** ± 3
Cheetah-run	305 ± 131	570 ± 253	640 ± 19	518 ± 28	660 ± 96	624 ± 10	**678** ± 46
Walker-walk	351 ± 58	897 ± 49	842 ± 51	902 ± 43	921 ± 45	938 ± 9	**953** ± 13
Cup-catch	460 ± 380	879 ± 87	852 ± 71	959 ± 27	963 ± 9	966 ± 9	**969** ± 5
100K step							
Finger-spin	136 ± 216	341 ± 70	693 ± 141	767 ± 56	901 ± 104	811 ± 146	**905** ± 57
Cartpole-swing	297 ± 39	326 ± 27	-	582 ± 146	**759** ± 92	373 ± 90	591 ± 55
Reacher-easy	20 ± 50	314 ± 155	-	538 ± 233	601 ± 213	567 ± 54	**722** ± 50
Cheetah-run	138 ± 88	235 ± 137	319 ± 56	299 ± 48	344 ± 67	381 ± 79	**413** ± 35
Walker-walk	224 ± 48	277 ± 12	361 ± 73	403 ± 24	612 ± 164	641 ± 89	**667** ± 147
Cup-catch	0 ± 0	246 ± 174	512 ± 110	769 ± 43	**913**± 53	666 ± 181	633 ± 241

Table 2: Performance on DeepMind Control Suite at 100K and 500K environment steps. The results show the mean and standard deviation averaged five runs, and the best results are indicated in bold. For baseline methods, we report the best numbers reported in prior works (Kostrikov et al., 2020).

three runs after 100K interactions (i.e., 400K frames with action repeat of 4). For our method, we consider a combination of sample-efficient versions of Rainbow DQN and SUNRISE (see Algorithm 3 in Appendix B). More experimental details and learning curves are in Appendix G.

For our method, we do not alter any hyperparameters of the original RL algorithms and train five ensemble agents. There are only three additional hyperparameters β, T, and λ for bootstrap, weighted Bellman backup, and UCB exploration, where we provide details in Appendix D, F, and G.

5.2 Comparative evaluation

OpenAI Gym. Table 1 shows the average returns of evaluation roll-outs for all methods. SUNRISE consistently improves the performance of SAC across all environments and outperforms the model-based RL methods, such as POPLIN-P and PETS, on all environments except Ant and SlimHumanoid-ET. Even though we focus on performance after small samples because of the recent emphasis on making RL more sample efficient, we find that the gain from SUNRISE becomes even more significant when training longer (see Figure 3(b) and Appendix D). We remark that SUNRISE is more compute-efficient than modern model-based RL methods, such as POPLIN and PETS, because they also utilize ensembles (of dynamics models) and perform planning to select actions. Namely, SUNRISE is simple to implement, computationally efficient, and readily parallelizable.

DeepMind Control Suite. As shown in Table 2, SUNRISE also consistently improves the performance of RAD (i.e., SAC with random crop) on all environments from DeepMind Control Suite. This implies that the proposed method can be useful for high-dimensional and complex input observations. Moreover, our method outperforms existing pixel-based RL methods in almost all environments. We remark that SUNRISE can also be combined with DrQ, and expect that it can achieve better performances on Cartpole-swing and Cup-catch at 100K environment steps.

Game	Human	Random	SimPLe	CURL	DrQ	Rainbow	SUNRISE
Alien	7127.7	227.8	616.9	558.2	761.4	789.0	**872.0**
Amidar	1719.5	5.8	88.0	**142.1**	97.3	118.5	122.6
Assault	742.0	222.4	527.2	**600.6**	489.1	413.0	594.8
Asterix	8503.3	210.0	**1128.3**	734.5	637.5	533.3	755.0
BankHeist	753.1	14.2	34.2	131.6	196.6	97.7	**266.7**
BattleZone	37187.5	2360.0	5184.4	14870.0	13520.6	7833.3	**15700.0**
Boxing	12.1	0.1	**9.1**	1.2	6.9	0.6	6.7
Breakout	30.5	1.7	**16.4**	4.9	14.5	2.3	1.8
ChopperCommand	7387.8	811.0	**1246.9**	1058.5	646.6	590.0	1040.0
CrazyClimber	35829.4	10780.5	**62583.6**	12146.5	19694.1	25426.7	22230.0
DemonAttack	1971.0	152.1	208.1	817.6	**1222.2**	688.2	919.8
Freeway	29.6	0.0	20.3	26.7	15.4	28.7	**30.2**
Frostbite	4334.7	65.2	254.7	1181.3	449.7	1478.3	**2026.7**
Gopher	2412.5	257.6	771.0	**669.3**	598.4	348.7	654.7
Hero	30826.4	1027.0	2656.6	6279.3	4001.6	3675.7	**8072.5**
Jamesbond	302.8	29.0	125.3	**471.0**	272.3	300.0	390.0
Kangaroo	3035.0	52.0	323.1	872.5	1052.4	1060.0	**2000.0**
Krull	2665.5	1598.0	**4539.9**	4229.6	4002.3	2592.1	3087.2
KungFuMaster	22736.3	258.5	**17257.2**	14307.8	7106.4	8600.0	10306.7
MsPacman	6951.6	307.3	1480.0	1465.5	1065.6	1118.7	**1482.3**
Pong	14.6	-20.7	**12.8**	-16.5	-11.4	-19.0	-19.3
PrivateEye	69571.3	24.9	58.3	**218.4**	49.2	97.8	100.0
Qbert	13455.0	163.9	1288.8	1042.4	1100.9	646.7	**1830.8**
RoadRunner	7845.0	11.5	5640.6	5661.0	8069.8	9923.3	**11913.3**
Seaquest	42054.7	68.4	**683.3**	384.5	321.8	396.0	570.7
UpNDown	11693.2	533.4	3350.3	2955.2	3924.9	3816.0	**5074.0**

Table 3: Performance on Atari games at 100K interactions. The results show the scores averaged three runs, and the best results are indicated in bold. For baseline methods, we report the best numbers reported in prior works (Kaiser et al., 2020; van Hasselt et al., 2019).

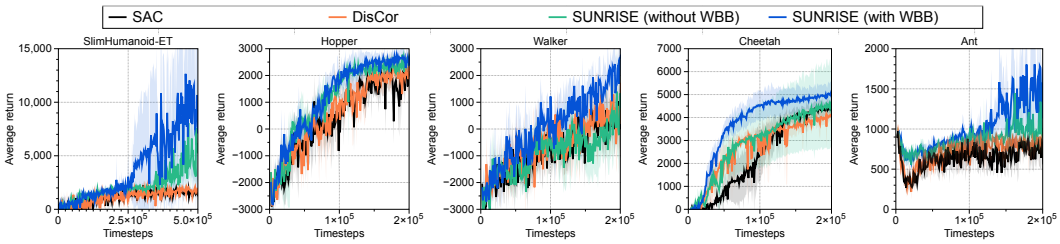

Figure 2: Learning curves on OpenAI Gym with noisy rewards. To verify the effects of the weighted Bellman backups (WBB), we consider SUNRISE with WBB and without WBB. The solid line and shaded regions represent the mean and standard deviation, respectively, across four runs.

Atari games. We also evaluate SUNRISE on discrete control tasks from the Atari benchmark using Rainbow DQN. Table 3 shows that SUNRISE improves the performance of Rainbow in almost all environments, and outperforms the state-of-the-art CURL and SimPLe on 11 out of 26 Atari games. Here, we remark that SUNRISE is also compatible with CURL, which could enable even better performance. These results demonstrate that SUNRISE is a general approach.

5.3 Ablation Study

Effects of weighted Bellman backups. To verify the effectiveness of the proposed weighted Bellman backup (4) in improving signal-to-noise in Q-updates, we evaluate on a modified OpenAI Gym environments with noisy rewards. Following Kumar et al. (2019), we add Gaussian noise to the reward function: $r'(s,a) = r(s,a) + z$, where $z \sim \mathcal{N}(0,1)$ only during training, and report the deterministic ground-truth reward during evaluation. For our method, we also consider a variant of SUNRISE, which updates Q-functions without the proposed weighted Bellman backup to isolate its effect. We compare to DisCor (Kumar et al., 2020), which improves SAC by reweighting the Bellman backup based on estimated cumulative Bellman errors (see Appendix E for more details).

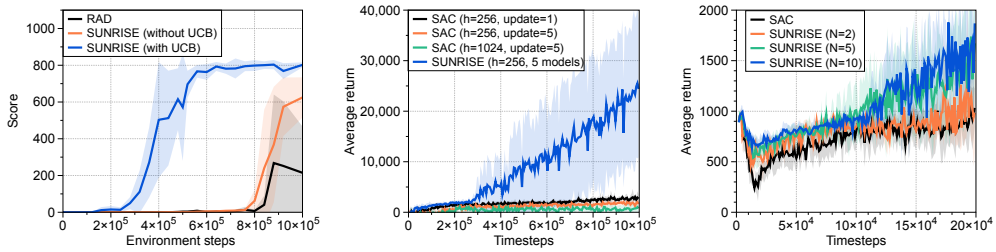

(a) Sparse reward (b) Gradient update (c) Ensemble size

Figure 3: (a) Effects of UCB exploration on the Cartpole environment with sparse reward. (b) Learning curves of SUNRISE and single agent with h hidden units and five gradient updates per each timestep on the SlimHumanoid-ET environment. (c) Learning curves of SUNRISE with varying values of ensemble size N on the Ant environment.

Figure 2 shows the learning curves of all methods on OpenAI Gym with noisy rewards. The proposed weighted Bellman backup significantly improves both sample-efficiency and asymptotic performance of SUNRISE, and outperforms baselines such as SAC and DisCor. We remark the performance gain due to our weighted Bellman backup becomes more significant in complex environments, such as SlimHumanoid-ET. These results imply that errors in the target Q-function can be characterized by the proposed confident weight in equation 5 effectively.

Effects of UCB exploration. To verify the advantage of UCB exploration in (6), we evaluate on Cartpole-swing with sparse-reward from DeepMind Control Suite. For our method, we consider a variant of SUNRISE, which selects action without UCB exploration. As shown in Fig 3(a), SUNRISE with UCB exploration (blue curve) significantly improves the sample-efficiency on the environment with sparse rewards.

Comparison with a single agent with more updates/parameters. One concern in utilizing the ensemble method is that its gains may come from more gradient updates and parameters. To clarify this concern, we compare SUNRISE (5 ensembles using 2-layer MLPs with 256 hidden units each) to a single agent, which consists of 2-layer MLPs with 1024 (and 256) hidden units with 5 updates using different random minibatches. Figure 3(b) shows that the learning curves on SlimHumanoid-ET, where SUNRISE outperforms all baselines. This implies that the gains from SUNRISE can not be achieved by simply increasing the number of updates/parameters. More experimental results on other environments are also available in Appendix D.

Effects of ensemble size. We analyze the effects of ensemble size N on the Ant environment from OpenAI Gym. Figure 3(c) shows that the performance can be improved by increasing the ensemble size, but the improvement is saturated around $N = 5$. Thus, we use five ensemble agents for all experiments. More experimental results on other environments are also available in Appendix D, where the overall trend is similar.

6 Conclusion

In this paper, we present the ensemble-based weighted Bellman backups, which is compatible with various off-policy RL algorithms. By re-weighting target Q-values based on uncertainty estimates, we stabilize and improve the learning process on both continuous and discrete control benchmarks. Additionally, we introduce SUNRISE, a simple unified ensemble method, which integrates the proposed weighted Bellman backups with bootstrap with random initialization, and UCB exploration to handle various issues in off-policy RL algorithms. Our experiments show that SUNRISE consistently improves the performances of existing off-policy RL algorithms, such as Soft Actor-Critic and Rainbow DQN, and outperforms state-of-the-art RL algorithms for both continuous and discrete control tasks on both low-dimensional and high-dimensional environments. We hope that SUNRISE could be useful to other relevant topics such as sim-to-real transfer (Tobin et al., 2017), imitation learning (Torabi et al., 2018), understanding the connection between on-policy and off-policy RL (Schulman et al., 2017), offline RL (Agarwal et al., 2020), and planning (Srinivas et al., 2018; Tamar et al., 2016).

REFERENCES

Rishabh Agarwal, Dale Schuurmans, and Mohammad Norouzi. An optimistic perspective on offline reinforcement learning. In *International Conference on Machine Learning*, 2020.

Brandon Amos, Samuel Stanton, Denis Yarats, and Andrew Gordon Wilson. On the model-based stochastic value gradient for continuous reinforcement learning. *arXiv preprint arXiv:2008.12775*, 2020.

Oron Anschel, Nir Baram, and Nahum Shimkin. Averaged-dqn: Variance reduction and stabilization for deep reinforcement learning. In *International Conference on Machine Learning*, 2017.

Peter Auer, Nicolo Cesa-Bianchi, and Paul Fischer. Finite-time analysis of the multiarmed bandit problem. *Machine learning*, 47(2-3):235–256, 2002.

Marc Bellemare, Sriram Srinivasan, Georg Ostrovski, Tom Schaul, David Saxton, and Remi Munos. Unifying count-based exploration and intrinsic motivation. In *Advances in Neural Information Processing Systems*, 2016.

Marc G Bellemare, Yavar Naddaf, Joel Veness, and Michael Bowling. The arcade learning environment: An evaluation platform for general agents. *Journal of Artificial Intelligence Research*, 47: 253–279, 2013.

Marc G Bellemare, Will Dabney, and Rémi Munos. A distributional perspective on reinforcement learning. In *International Conference on Machine Learning*, 2017.

Greg Brockman, Vicki Cheung, Ludwig Pettersson, Jonas Schneider, John Schulman, Jie Tang, and Wojciech Zaremba. Openai gym. *arXiv preprint arXiv:1606.01540*, 2016.

Richard Y Chen, Szymon Sidor, Pieter Abbeel, and John Schulman. Ucb exploration via q-ensembles. *arXiv preprint arXiv:1706.01502*, 2017.

Jongwook Choi, Yijie Guo, Marcin Moczulski, Junhyuk Oh, Neal Wu, Mohammad Norouzi, and Honglak Lee. Contingency-aware exploration in reinforcement learning. In *International Conference on Learning Representations*, 2019.

Kurtland Chua, Roberto Calandra, Rowan McAllister, and Sergey Levine. Deep reinforcement learning in a handful of trials using probabilistic dynamics models. In *Advances in Neural Information Processing Systems*, 2018.

Bradley Efron. *The jackknife, the bootstrap, and other resampling plans*, volume 38. Siam, 1982.

Scott Fujimoto, Herke Van Hoof, and David Meger. Addressing function approximation error in actor-critic methods. In *International Conference on Machine Learning*, 2018.

Tuomas Haarnoja, Aurick Zhou, Pieter Abbeel, and Sergey Levine. Soft actor-critic: Off-policy maximum entropy deep reinforcement learning with a stochastic actor. In *International Conference on Machine Learning*, 2018.

Danijar Hafner, Timothy Lillicrap, Ian Fischer, Ruben Villegas, David Ha, Honglak Lee, and James Davidson. Learning latent dynamics for planning from pixels. In *International Conference on Machine Learning*, 2019.

Danijar Hafner, Timothy Lillicrap, Jimmy Ba, and Mohammad Norouzi. Dream to control: Learning behaviors by latent imagination. In *International Conference on Learning Representations*, 2020.

Hado V Hasselt. Double q-learning. In *Advances in Neural Information Processing Systems*, 2010.

Matteo Hessel, Joseph Modayil, Hado Van Hasselt, Tom Schaul, Georg Ostrovski, Will Dabney, Dan Horgan, Bilal Piot, Mohammad Azar, and David Silver. Rainbow: Combining improvements in deep reinforcement learning. In *AAAI Conference on Artificial Intelligence*, 2018.

Rein Houthooft, Xi Chen, Yan Duan, John Schulman, Filip De Turck, and Pieter Abbeel. Vime: Variational information maximizing exploration. In *Advances in Neural Information Processing Systems*, 2016.

Lukasz Kaiser, Mohammad Babaeizadeh, Piotr Milos, Blazej Osinski, Roy H Campbell, Konrad Czechowski, Dumitru Erhan, Chelsea Finn, Piotr Kozakowski, Sergey Levine, et al. Model-based reinforcement learning for atari. In *International Conference on Learning Representations*, 2020.

Dmitry Kalashnikov, Alex Irpan, Peter Pastor, Julian Ibarz, Alexander Herzog, Eric Jang, Deirdre Quillen, Ethan Holly, Mrinal Kalakrishnan, Vincent Vanhoucke, et al. Qt-opt: Scalable deep reinforcement learning for vision-based robotic manipulation. In *Conference on Robot Learning*, 2018.

Ilya Kostrikov, Denis Yarats, and Rob Fergus. Image augmentation is all you need: Regularizing deep reinforcement learning from pixels. *arXiv preprint arXiv:2004.13649*, 2020.

Aviral Kumar, Justin Fu, Matthew Soh, George Tucker, and Sergey Levine. Stabilizing off-policy q-learning via bootstrapping error reduction. In *Advances in Neural Information Processing Systems*, 2019.

Aviral Kumar, Abhishek Gupta, and Sergey Levine. Discor: Corrective feedback in reinforcement learning via distribution correction. In *Advances in Neural Information Processing Systems*, 2020.

Thanard Kurutach, Ignasi Clavera, Yan Duan, Aviv Tamar, and Pieter Abbeel. Model-ensemble trust-region policy optimization. In *International Conference on Learning Representations*, 2018.

Qingfeng Lan, Yangchen Pan, Alona Fyshe, and Martha White. Maxmin q-learning: Controlling the estimation bias of q-learning. In *International Conference on Learning Representations*, 2020.

Michael Laskin, Kimin Lee, Adam Stooke, Lerrel Pinto, Pieter Abbeel, and Aravind Srinivas. Reinforcement learning with augmented data. In *Advances in Neural Information Processing Systems*, 2020.

Alex X Lee, Anusha Nagabandi, Pieter Abbeel, and Sergey Levine. Stochastic latent actor-critic: Deep reinforcement learning with a latent variable model. In *Advances in Neural Information Processing Systems*, 2020.

Volodymyr Mnih, Koray Kavukcuoglu, David Silver, Andrei A Rusu, Joel Veness, Marc G Bellemare, Alex Graves, Martin Riedmiller, Andreas K Fidjeland, Georg Ostrovski, et al. Human-level control through deep reinforcement learning. *Nature*, 518(7540):529, 2015.

Ian Osband, Charles Blundell, Alexander Pritzel, and Benjamin Van Roy. Deep exploration via bootstrapped dqn. In *Advances in Neural Information Processing Systems*, 2016.

Deepak Pathak, Pulkit Agrawal, Alexei A Efros, and Trevor Darrell. Curiosity-driven exploration by self-supervised prediction. In *International Conference on Machine Learning*, 2017.

Tom Schaul, John Quan, Ioannis Antonoglou, and David Silver. Prioritized experience replay. In *International Conference on Learning Representations*, 2016.

John Schulman, Sergey Levine, Pieter Abbeel, Michael Jordan, and Philipp Moritz. Trust region policy optimization. In *International Conference on Machine Learning*, 2015.

John Schulman, Xi Chen, and Pieter Abbeel. Equivalence between policy gradients and soft q-learning. *arXiv preprint arXiv:1704.06440*, 2017.

David Silver, Julian Schrittwieser, Karen Simonyan, Ioannis Antonoglou, Aja Huang, Arthur Guez, Thomas Hubert, Lucas Baker, Matthew Lai, Adrian Bolton, et al. Mastering the game of go without human knowledge. *Nature*, 550(7676):354, 2017.

David Silver, Thomas Hubert, Julian Schrittwieser, Ioannis Antonoglou, Matthew Lai, Arthur Guez, Marc Lanctot, Laurent Sifre, Dharshan Kumaran, Thore Graepel, et al. A general reinforcement learning algorithm that masters chess, shogi, and go through self-play. *Science*, 362(6419):1140–1144, 2018.

Aravind Srinivas, Allan Jabri, Pieter Abbeel, Sergey Levine, and Chelsea Finn. Universal planning networks. In *International Conference on Machine Learning*, 2018.

Aravind Srinivas, Michael Laskin, and Pieter Abbeel. Curl: Contrastive unsupervised representations for reinforcement learning. In *International Conference on Machine Learning*, 2020.

Aviv Tamar, Yi Wu, Garrett Thomas, Sergey Levine, and Pieter Abbeel. Value iteration networks. In *Advances in Neural Information Processing Systems*, 2016.

Yuval Tassa, Yotam Doron, Alistair Muldal, Tom Erez, Yazhe Li, Diego de Las Casas, David Budden, Abbas Abdolmaleki, Josh Merel, Andrew Lefrancq, et al. Deepmind control suite. *arXiv preprint arXiv:1801.00690*, 2018.

Josh Tobin, Rachel Fong, Alex Ray, Jonas Schneider, Wojciech Zaremba, and Pieter Abbeel. Domain randomization for transferring deep neural networks from simulation to the real world. In *International Conference on Intelligent Robots and Systems*, 2017.

Faraz Torabi, Garrett Warnell, and Peter Stone. Behavioral cloning from observation. In *International Joint Conferences on Artificial Intelligence Organization*, 2018.

Hado Van Hasselt, Arthur Guez, and David Silver. Deep reinforcement learning with double q-learning. In *AAAI Conference on Artificial Intelligence*, 2016.

Hado P van Hasselt, Matteo Hessel, and John Aslanides. When to use parametric models in reinforcement learning? In *Advances in Neural Information Processing Systems*, 2019.

Oriol Vinyals, Igor Babuschkin, Wojciech M Czarnecki, Michael Mathieu, Andrew Dudzik, Junyoung Chung, David H Choi, Richard Powell, Timo Ewalds, Petko Georgiev, et al. Grandmaster level in starcraft ii using multi-agent reinforcement learning. *Nature*, 575(7782):350–354, 2019.

Tingwu Wang and Jimmy Ba. Exploring model-based planning with policy networks. In *International Conference on Learning Representations*, 2020.

Tingwu Wang, Xuchan Bao, Ignasi Clavera, Jerrick Hoang, Yeming Wen, Eric Langlois, Shunshi Zhang, Guodong Zhang, Pieter Abbeel, and Jimmy Ba. Benchmarking model-based reinforcement learning. *arXiv preprint arXiv:1907.02057*, 2019.

Marco A Wiering and Hado Van Hasselt. Ensemble algorithms in reinforcement learning. *IEEE Transactions on Systems, Man, and Cybernetics*, 38(4):930–936, 2008.

Denis Yarats, Amy Zhang, Ilya Kostrikov, Brandon Amos, Joelle Pineau, and Rob Fergus. Improving sample efficiency in model-free reinforcement learning from images. *arXiv preprint arXiv:1910.01741*, 2019.

Brian D Ziebart. Modeling purposeful adaptive behavior with the principle of maximum causal entropy. 2010.

Appendix

A SUNRISE: SOFT ACTOR-CRITIC

Background. SAC (Haarnoja et al., 2018) is a state-of-the-art off-policy algorithm for continuous control problems. SAC learns a policy, $\pi_\phi(a|s)$, and a critic, $Q_\theta(s,a)$, and aims to maximize a weighted objective of the reward and the policy entropy, $\mathbb{E}_{s_t,a_t\sim\pi}\left[\sum_t \gamma^{t-1} r_t + \alpha\mathcal{H}(\pi_\phi(\cdot|s_t))\right]$. To update the parameters, SAC alternates between a soft policy evaluation and a soft policy improvement. At the soft policy evaluation step, a soft Q-function, which is modeled as a neural network with parameters θ, is updated by minimizing the following soft Bellman residual:

$$\mathcal{L}^{\texttt{SAC}}_{\texttt{critic}}(\theta) = \mathbb{E}_{\tau_t\sim\mathcal{B}}[\mathcal{L}_Q(\tau_t,\theta)],$$
$$\mathcal{L}_Q(\tau_t,\theta) = \left(Q_\theta(s_t,a_t) - r_t - \gamma\mathbb{E}_{a_{t+1}\sim\pi_\phi}\left[Q_{\bar{\theta}}(s_{t+1},a_{t+1}) - \alpha\log\pi_\phi(a_{t+1}|s_{t+1})\right]\right)^2,$$

where $\tau_t = (s_t, a_t, r_t, s_{t+1})$ is a transition, $\mathcal{B}$ is a replay buffer, $\bar{\theta}$ are the delayed parameters, and α is a temperature parameter. At the soft policy improvement step, the policy π with its parameter ϕ is updated by minimizing the following objective:

$$\mathcal{L}^{\texttt{SAC}}_{\texttt{actor}}(\phi) = \mathbb{E}_{s_t\sim\mathcal{B}}\left[\mathcal{L}_\pi(s_t,\phi)\right], \text{ where } \mathcal{L}_\pi(s_t,\phi) = \mathbb{E}_{a_t\sim\pi_\phi}\left[\alpha\log\pi_\phi(a_t|s_t) - Q_\theta(s_t,a_t)\right].$$

We remark that this corresponds to minimizing the Kullback-Leibler divergence between the policy and a Boltzmann distribution induced by the current soft Q-function.

SUNRISE without UCB exploration. For SUNRISE without UCB exploration, we use random inference proposed in Bootstrapped DQN (Osband et al., 2016), which randomly selects an index of policy uniformly at random and generates the action from the selected actor for the duration of that episode (see Line 3 in Algorithm 2).

Algorithm 2 SUNRISE: SAC version (random inference)

1: **for** each iteration **do**
2: // RANDOM INFERENCE
3: Select an index of policy using $\widehat{i} \sim \text{Uniform}\{1,\cdots,N\}$
4: **for** each timestep t **do**
5: Get the action from selected policy: $a_t \sim \pi_{\phi_{\widehat{i}}}(a|s_t)$
6: Collect state s_{t+1} and reward r_t from the environment by taking action a_t
7: Sample bootstrap masks $M_t = \{m_{t,i} \sim \text{Bernoulli}\,(\beta) \text{ — } i \in \{1,\ldots,N\}\}$
8: Store transitions $\tau_t = (s_t, a_t, s_{t+1}, r_t)$ and masks in replay buffer $\mathcal{B} \leftarrow \mathcal{B} \cup \{(\tau_t, M_t)\}$
9: **end for**
10: // UPDATE AGENTS VIA BOOTSTRAP AND WEIGHTED BELLMAN BACKUP
11: **for** each gradient step **do**
12: Sample random minibatch $\{(\tau_j, M_j)\}_{j=1}^B \sim \mathcal{B}$
13: **for** each agent i **do**
14: Update the Q-function by minimizing $\frac{1}{B}\sum_{j=1}^B m_{j,i}\mathcal{L}_{WQ}(\tau_j,\theta_i)$
15: Update the policy by minimizing $\frac{1}{B}\sum_{j=1}^B m_{j,i}\mathcal{L}_\pi(s_j,\phi_i)$
16: **end for**
17: **end for**
18: **end for**

B EXTENSION TO RAINBOW DQN

B.1 PRELIMINARIES: RAINBOW DQN

Background. DQN algorithm (Mnih et al., 2015) learns a Q-function, which is modeled as a neural network with parameters θ, by minimizing the following Bellman residual:

$$\mathcal{L}^{\texttt{DQN}}(\theta) = \mathbb{E}_{\tau_t\sim\mathcal{B}}\left[\left(Q_\theta(s_t,a_t) - r_t - \gamma\max_a Q_{\bar{\theta}}(s_{t+1},a)\right)^2\right], \tag{7}$$

where $\tau_t = (s_t, a_t, r_t, s_{t+1})$ is a transition, $\mathcal{B}$ is a replay buffer, and $\bar{\theta}$ are the delayed parameters. Even though Rainbow DQN integrates several techniques, such as double Q-learning (Van Hasselt et al., 2016) and distributional DQN (Bellemare et al., 2017), applying SUNRISE to Rainbow DQN can be described based on the standard DQN algorithm. For exposition, we refer the reader to Hessel et al. (2018) for more detailed explanations of Rainbow DQN.

Algorithm 3 SUNRISE: Rainbow version

for each iteration **do**
  for each timestep t **do**
    // UCB EXPLORATION
    Choose the action that maximizes UCB: $a_t = \arg\max_{a_{t,i} \in \mathcal{A}} Q_{\texttt{mean}}(s_t, a_{t,i}) + \lambda Q_{\texttt{std}}(s_t, a_{t,i})$
    Collect state s_{t+1} and reward r_t from the environment by taking action a_t
    Sample bootstrap masks $M_t = \{m_{t,i} \sim \text{Bernoulli}\,(\beta) \text{ — } i \in \{1, \ldots, N\}\}$
    Store transitions $\tau_t = (s_t, a_t, s_{t+1}, r_t)$ and masks in replay buffer $\mathcal{B} \leftarrow \mathcal{B} \cup \{(\tau_t, M_t)\}$
  end for
  // UPDATE Q-FUNCTIONS VIA BOOTSTRAP AND WEIGHTED BELLMAN BACKUP
  for each gradient step **do**
    Sample random minibatch $\{(\tau_j, M_j)\}_{j=1}^{B} \sim \mathcal{B}$
    for each agent i **do**
      Update the Q-function by minimizing $\frac{1}{B}\sum_{j=1}^{B} m_{j,i} \mathcal{L}_{WQ}^{\texttt{DQN}}(\tau_j, \theta_i)$
    end for
  end for
end for

B.2 SUNRISE: RAINBOW DQN

Bootstrap with random initialization. Formally, we consider an ensemble of N Q-functions, i.e., $\{Q_{\theta_i}\}_{i=1}^{N}$, where θ_i denotes the parameters of the i-th Q-function.[3] To train the ensemble of Q-functions, we use the bootstrap with random initialization (Efron, 1982; Osband et al., 2016), which enforces the diversity between Q-functions through two simple ideas: First, we initialize the model parameters of all Q-functions with random parameter values for inducing an initial diversity in the models. Second, we apply different samples to train each Q-function. Specifically, for each Q-function i in each timestep t, we draw the binary masks $m_{t,i}$ from the Bernoulli distribution with parameter $\beta \in (0, 1]$, and store them in the replay buffer. Then, when updating the model parameters of Q-functions, we multiply the bootstrap mask to each objective function.

Weighted Bellman backup. Since conventional Q-learning is based on the Bellman backup in equation 7, it can be affected by error propagation. I.e., error in the target Q-function $Q_{\bar{\theta}}(s_{t+1}, a_{t+1})$ gets propagated into the Q-function $Q_\theta(s_t, a_t)$ at the current state. Recently, Kumar et al. (2020) showed that this error propagation can cause inconsistency and unstable convergence. To mitigate this issue, for each Q-function i, we consider a weighted Bellman backup as follows:

$$\mathcal{L}_{WQ}^{\texttt{DQN}}(\tau_t, \theta_i) = w(s_{t+1}) \left(Q_{\theta_i}(s_t, a_t) - r_t - \gamma \max_a Q_{\bar{\theta}_i}(s_{t+1}, a) \right)^2,$$

where $\tau_t = (s_t, a_t, r_t, s_{t+1})$ is a transition, and $w(s)$ is a confidence weight based on ensemble of target Q-functions:

$$w(s) = \sigma\left(-\bar{Q}_{\texttt{std}}(s) * T\right) + 0.5, \tag{8}$$

where $T > 0$ is a temperature, σ is the sigmoid function, and $\bar{Q}_{\texttt{std}}(s)$ is the empirical standard deviation of all target Q-functions $\{\max_a Q_{\bar{\theta}_i}(s, a)\}_{i=1}^{N}$. Note that the confidence weight is bounded in $[0.5, 1.0]$ because standard deviation is always positive.[4] The proposed objective $\mathcal{L}_{WQ}^{\texttt{DQN}}$ down-weights the sample transitions with high variance across target Q-functions, resulting in a loss function for the Q-updates that has a better signal-to-noise ratio. Note that we combine the proposed

[3] Here, we remark that each Q-function has a unique target Q-function.

[4] We find that it is empirically stable to set minimum value of weight $w(s, a)$ as 0.5.

weighted Bellman backup with prioritized replay (Schaul et al., 2016) by multiplying both weights to Bellman backups.

UCB exploration. The ensemble can also be leveraged for efficient exploration (Chen et al., 2017; Osband et al., 2016) because it can express higher uncertainty on unseen samples. Motivated by this, by following the idea of Chen et al. (2017), we consider an optimism-based exploration that chooses the action that maximizes

$$a_t = \max_a \{Q_{\texttt{mean}}(s_t, a) + \lambda Q_{\texttt{std}}(s_t, a)\}, \tag{9}$$

where $Q_{\texttt{mean}}(s, a)$ and $Q_{\texttt{std}}(s, a)$ are the empirical mean and standard deviation of all Q-functions $\{Q_{\theta_i}\}_{i=1}^N$, and the $\lambda > 0$ is a hyperparameter. This inference method can encourage exploration by adding an exploration bonus (i.e., standard deviation $Q_{\texttt{std}}$) for visiting unseen state-action pairs similar to the UCB algorithm (Auer et al., 2002). This inference method was originally proposed in Chen et al. (2017) for efficient exploration in DQN, but we further extend it to Rainbow DQN. For evaluation, we approximate the maximum a posterior action by choosing the action maximizes the mean of Q-functions, i.e., $a_t = \max_a \{Q_{\texttt{mean}}(s_t, a)\}$. The full procedure is summarized in Algorithm 3.

C Implementation details for toy regression tasks

We evaluate the quality of uncertainty estimates from an ensemble of neural networks on a toy regression task. To this end, we generate twenty training samples drawn as $y = x^3 + \epsilon$, where $\epsilon \sim \mathcal{N}(0, 3^2)$, and train ten ensembles of regression networks using bootstrap with random initialization. The regression network is as fully-connected neural networks with 2 hidden layers and 50 rectified linear units in each layer. For bootstrap, we draw the binary masks from the Bernoulli distribution with mean $\beta = 0.3$. As uncertainty estimates, we measure the empirical variance of the networks' predictions. As shown in Figure 1(b), the ensemble can produce well-calibrated uncertainty estimates (i.e., variance) on unseen samples.

D Experimental setups and results: OpenAI Gym

Environments. We evaluate the performance of SUNRISE on four complex environments based on the standard bench-marking environments[5] from OpenAI Gym (Brockman et al., 2016). Note that we do not use a modified Cheetah environments from PETS (Chua et al., 2018) (dented as Cheetah in POPLIN (Wang & Ba, 2020)) because it includes additional information in observations.

Training details. We consider a combination of SAC and SUNRISE using the publicly released implementation repository (https://github.com/vitchyr/rlkit) without any modifications on hyperparameters and architectures. For our method, the temperature for weighted Bellman backups is chosen from $T \in \{10, 20, 50\}$, the mean of the Bernoulli distribution is chosen from $\beta \in \{0.5, 1.0\}$, the penalty parameter is chosen from $\lambda \in \{1, 5, 10\}$, and we train five ensemble agents. The optimal parameters are chosen to achieve the best performance on training environments. Here, we remark that training ensemble agents using same training samples but with different initialization (i.e., $\beta = 1$) usually achieves the best performance in most cases similar to Osband et al. (2016) and Chen et al. (2017). We expect that this is because splitting samples can reduce the sample-efficiency. Also, initial diversity from random initialization can be enough because each Q-function has a unique target Q-function, i.e., target value is also different according to initialization.

Learning curves. Figure 4 shows the learning curves on all environments. One can note that SUNRISE consistently improves the performance of SAC by a large margin.

Effects of ensembles. Figure 5 shows the learning curves of SUNRISE with varying values of ensemble size on all environments. The performance can be improved by increasing the ensemble size, but the improvement is saturated around $N = 5$.

[5] We used the reference implementation at https://github.com/WilsonWangTHU/mbbl (Wang et al., 2019).

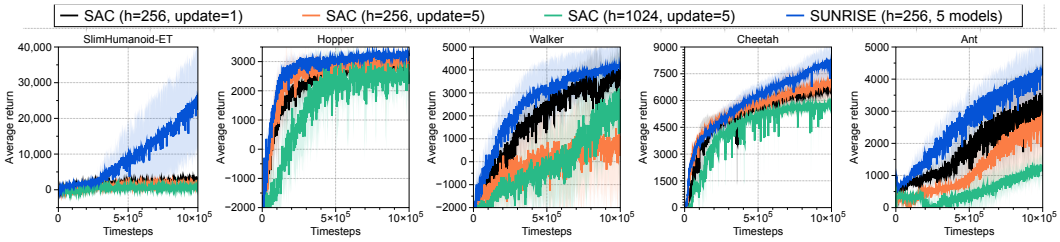

Figure 4: Learning curves of SUNRISE and single agent with h hidden units and five gradient updates per each timestep on OpenAI Gym. The solid line and shaded regions represent the mean and standard deviation, respectively, across four runs.

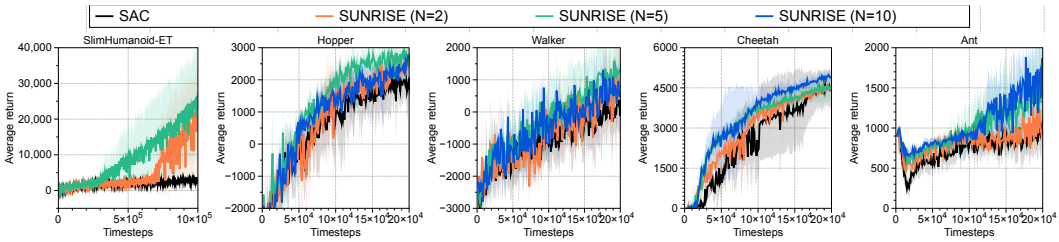

Figure 5: Learning curves of SUNRISE with varying values of ensemble size N. The solid line and shaded regions represent the mean and standard deviation, respectively, across four runs.

E EXPERIMENTAL SETUPS AND RESULTS: NOISY REWARD

DisCor. DisCor (Kumar et al., 2020) was proposed to prevent the error propagation issue in Q-learning. In addition to a standard Q-learning, DisCor trains an error model $\Delta_\psi(s, a)$, which approximates the cumulative sum of discounted Bellman errors over the past iterations of training. Then, using the error model, DisCor reweights the Bellman backups based on a confidence weight defined as follows:

$$w(s, a) \propto \exp\left(-\frac{\gamma \Delta_\psi(s, a)}{T}\right),$$

where γ is a discount factor and T is a temperature. By following the setups in Kumar et al. (2020), we take a network with 1 extra hidden layer than the corresponding Q-network as an error model, and chose $T = 10$ for all experiments. We update the temperature via a moving average and use the learning rate of 0.0003. We use the SAC algorithm as the RL objective coupled with DisCor and build on top of the publicly released implementation repository (https://github.com/vitchyr/rlkit).

Hyperparameter	Value	Hyperparameter	Value
Random crop	True	Initial temperature	0.1
Observation rendering	$(100, 100)$	Learning rate $(f_\theta, \pi_\psi, Q_\phi)$	$2e-4$ cheetah, run
Observation downsampling	$(84, 84)$		$1e-3$ otherwise
Replay buffer size	100000	Learning rate (α)	$1e-4$
Initial steps	1000	Batch Size	512 (cheetah), 256 (rest)
Stacked frames	3	Q function EMA τ	0.01
Action repeat	2 finger, spin; walker, walk	Critic target update freq	2
	8 cartpole, swingup	Convolutional layers	4
	4 otherwise	Number of filters	32
Hidden units (MLP)	1024	Non-linearity	ReLU
Evaluation episodes	10	Encoder EMA τ	0.05
Optimizer	Adam	Latent dimension	50
$(\beta_1, \beta_2) \rightarrow (f_\theta, \pi_\psi, Q_\phi)$	$(.9, .999)$	Discount γ	.99
$(\beta_1, \beta_2) \rightarrow (\alpha)$	$(.5, .999)$		

Table 4: Hyperparameters used for DeepMind Control Suite experiments. Most hyperparameters values are unchanged across environments with the exception for action repeat, learning rate, and batch size.

F Experimental setups and results: DeepMind Control Suite

Training details. We consider a combination of RAD and SUNRISE using the publicly released implementation repository (https://github.com/MishaLaskin/rad) with a full list of hyperparameters in Table 4. Similar to Laskin et al. (2020), we use the same encoder architecture as in (Yarats et al., 2019), and the actor and critic share the same encoder to embed image observations.[6] For our method, the temperature for weighted Bellman backups is chosen from $T \in \{10, 100\}$, the mean of the Bernoulli distribution is chosen from $\beta \in \{0.5, 1.0\}$, the penalty parameter is chosen from $\lambda \in \{1, 5, 10\}$, and we train five ensemble agents. The optimal parameters are chosen to achieve the best performance on training environments. Here, we remark that training ensemble agents using same training samples but with different initialization (i.e., $\beta = 1$) usually achieves the best performance in most cases similar to Osband et al. (2016) and Chen et al. (2017). We expect that this is because training samples can reduce the sample-efficiency. Also, initial diversity from random initialization can be enough because each Q-function has a unique target Q-function, i.e., target value is also different according to initialization.

Learning curves. Figure 6(g), 6(h), 6(i), 6(j), 6(k), and 6(l) show the learning curves on all environments. Since RAD already achieves the near optimal performances and the room for improvement is small, we can see a small but consistent gains from SUNRISE. To verify the effectiveness of SUNRISE more clearly, we consider a combination of SAC and SUNRISE in Figure 6(a), 6(b), 6(c), 6(d), 6(e), and 6(f), where the gain from SUNRISE is more significant.

G Experimental setups and results: Atari games

Training details. We consider a combination of sample-efficient versions of Rainbow DQN and SUNRISE using the publicly released implementation repository (https://github.com/Kaixhin/Rainbow) without any modifications on hyperparameters and architectures. For our method, the temperature for weighted Bellman backups is chosen from $T \in \{10, 40\}$, the mean of the Bernoulli distribution is chosen from $\beta \in \{0.5, 1.0\}$, the penalty parameter is chosen from $\lambda \in \{1, 10\}$, and we train five ensemble agents. The optimal parameters are chosen to achieve the best performance on training environments. Here, we remark that training ensemble agents using same training samples but with different initialization (i.e., $\beta = 1$) usually achieves the best performance in most cases similar to Osband et al. (2016) and Chen et al. (2017). We expect that this is because splitting samples can reduce the sample-efficiency. Also, initial diversity from random initialization can be enough because each Q-function has a unique target Q-function, i.e., target value is also different according to initialization.

[6] However, we remark that each agent does not share the encoders unlike Bootstrapped DQN (Osband et al., 2016).

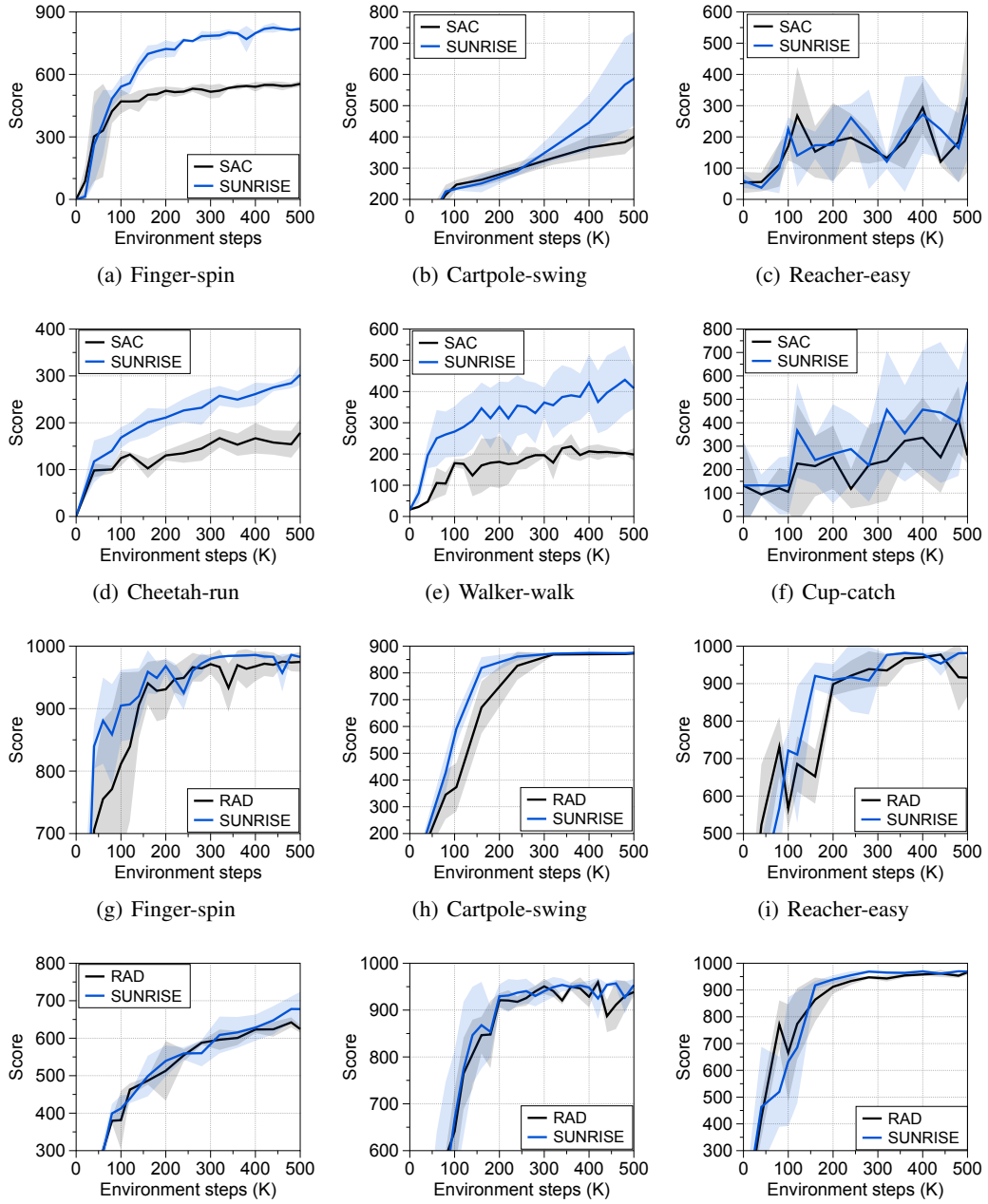

(a) Finger-spin (b) Cartpole-swing (c) Reacher-easy

(d) Cheetah-run (e) Walker-walk (f) Cup-catch

(g) Finger-spin (h) Cartpole-swing (i) Reacher-easy

(j) Cheetah-run (k) Walker-walk (l) Cup-catch

Figure 6: Learning curves of (a-f) SAC and (g-I) RAD on DeepMind Control Suite. The solid line and shaded regions represent the mean and standard deviation, respectively, across five runs.

Learning curves. Figure 7, Figure 8 and Figure 9 show the learning curves on all environments.

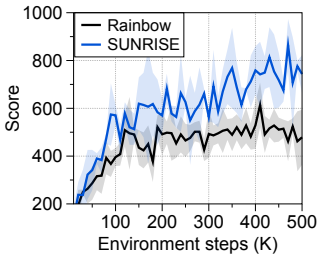

(a) Seaquest

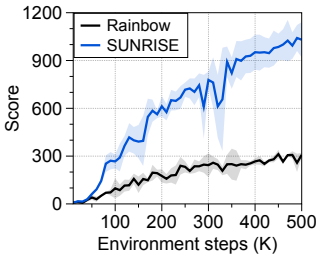

(b) BankHeist

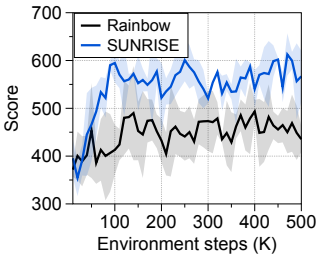

(c) Assualt

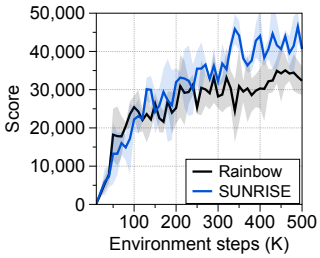

(d) CrazyClimber

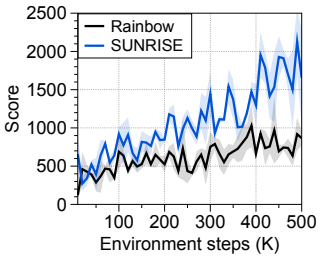

(e) DemonAttack

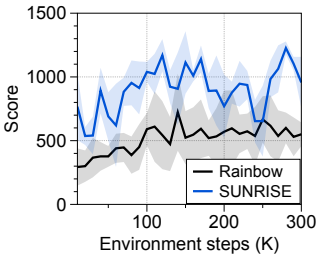

(f) ChopperCommand

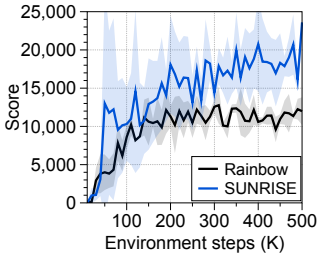

(g) KungFuMaster

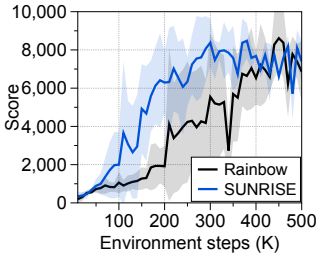

(h) Kangaroo

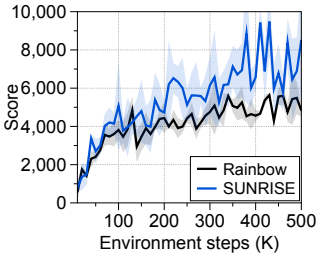

(i) UpNDown

Figure 7: Learning curves on Atari games. The solid line and shaded regions represent the mean and standard deviation, respectively, across three runs.

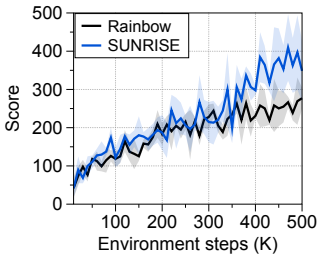

(a) Amidar

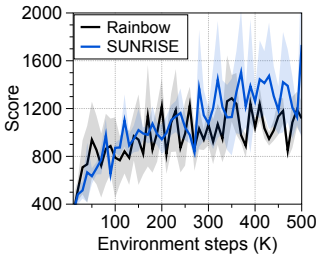

(b) Alien

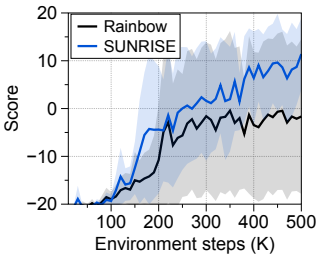

(c) Pong

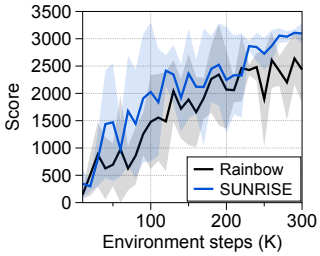

(d) Frostbite

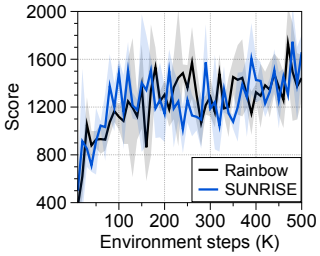

(e) MsPacman

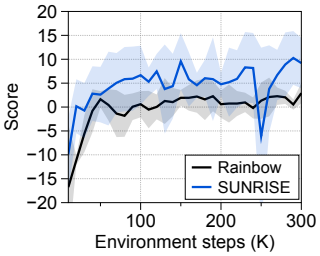

(f) Boxing

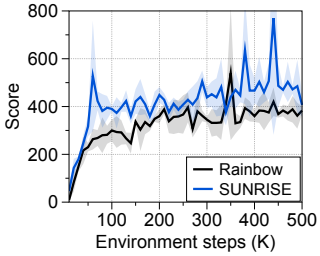

(g) Jamesbond

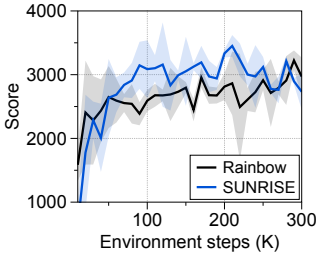

(h) Krull

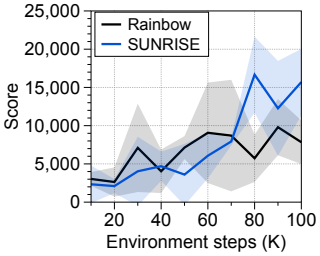

(i) BattleZone

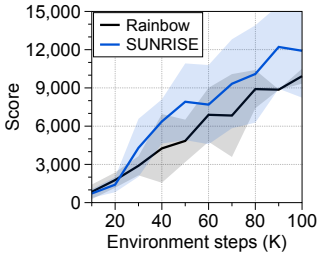

(j) RoadRunner

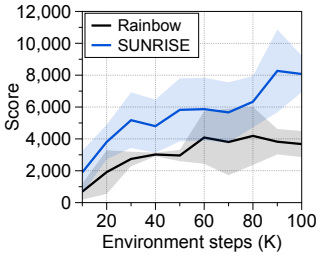

(k) Hero

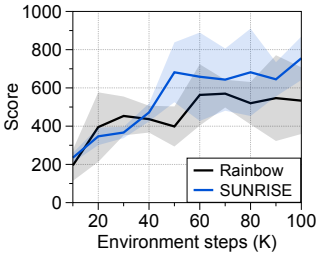

(l) Asterix

Figure 8: Learning curves on Atari games. The solid line and shaded regions represent the mean and standard deviation, respectively, across three runs.

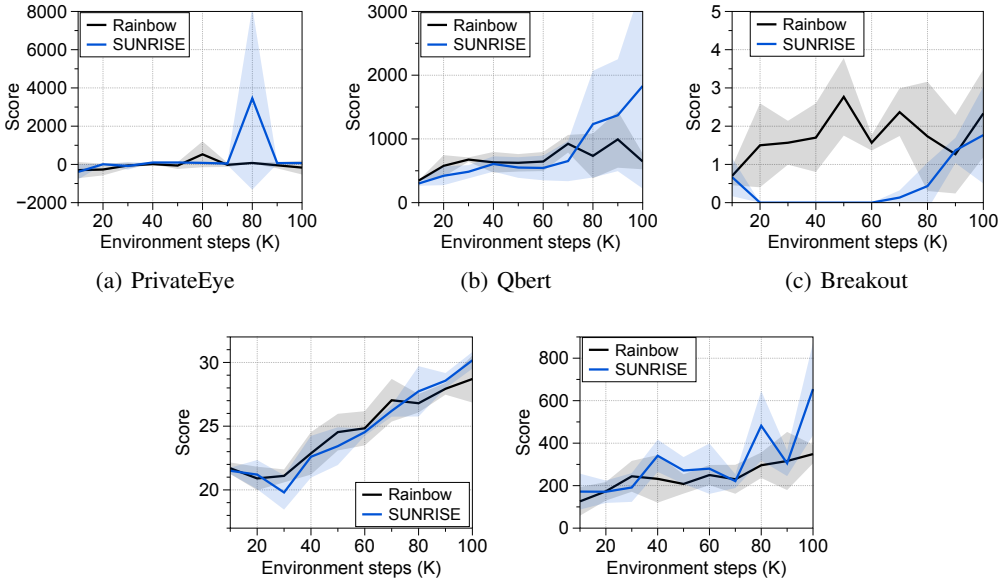

(a) PrivateEye (b) Qbert (c) Breakout

(d) Freeway (e) Gopher

Figure 9: Learning curves on Atari games. The solid line and shaded regions represent the mean and standard deviation, respectively, across three runs.